Title: Engineering bacterial blight-resistant plants through CRISPR/Cas9-targeted editing of the *MeSWEET10a* promoter in cassava

Yajie Wang[1,2,4], Mengting Geng[2,4], Ranran Pan[3,4], Tong Zhang[2], Xinghou Zhen[2], Yannian Che[2], Ruimei Li[1], Jiao Liu[1], Yinhua Chen*[2], Jianchun Guo*[1], Yuan Yao*[1]

[1]Key Laboratory of Biology and Genetic Resources of Tropical Crops, Ministry of Agriculture, Institute of Tropical Bioscience and Biotechnology, Chinese Academy of Tropical Agricultural Sciences, Haikou, China

[2]Hainan Key Laboratory for Sustainable Utilization of Tropical Bioresource, Hainan University, Haikou, China

[3]College of Agriculture & Biotechnology, Zhejiang University, Hangzhou, China

[4]These authors contributed equally to the article.

***Correspondence: Yinhua Chen** (yhchen@hainu.edu.cn), **Jianchun Guo** (guojianchun@itbb.org.cn), **Yuan Yao** (yaoyuan@itbb.org.cn)

Abstract:

Editing of the promoter in the disease-susceptibility gene *MeSWEET10a* of SC8 cassava confers resistance to cassava bacterial blight (CBB). All mutated cassava lines had normal morphological and yield-related traits as the wild type. The results lay a research foundation for breeding cassava resistant to bacterial blight.

22 Dear Editor,

23 Cassava (*Manihot esculenta* Crantz) is a major food crop in tropical and
24 subtropical regions that provides food security for 800 million people. However,
25 cassava bacterial blight (CBB) caused by *Xanthomonas axonopodis* pv. *manihotis*
26 (*Xam*) results in severe yield losses and is the most destructive bacterial disease in all
27 worldwide cassava planting regions (McCallum et al., 2017). The vast majority of
28 cassava cultivars are not resistant to CBB. *Xam* pathogen infection secretes
29 transcription activator-like effectors (TALEs) into cassava host cells through the type
30 III secretion system (Boch and Bonas, 2010). The repeat variable diresidues (RVDs)
31 in TALEs recognize the effector-binding elements (EBEs) on the host susceptibility
32 (S) gene promoters and activate S gene expression which facilitates bacterial growth
33 and disease symptom formation.

34 Inhibition of S gene expression by genetic engineering is an attractive strategy to
35 improve plant disease resistance (Zaidi et al., 2018). *Mildew resistance locus O* (*Mlo*)
36 is one of the best-known S genes and encodes a conserved membrane-associated
37 protein. Mlo is required for the penetration of powdery mildew (PM) fungi into host
38 epidermal cells. Mutation of *Mlo* through CRISPR-Cas9 has conferred PM resistance
39 in wheat (Wang et al., 2014). In addition, mutations of other S genes such as *eIF4E*
40 and *MPK* enhances disease resistance (Gomez et al., 2019; Xie and Yang, 2013).
41 However, these mutations often affect plant fitness with reduced growth, fertility,
42 yield, and abiotic stress tolerance (Zaidi et al., 2018). Genetic engineering of the core
43 S gene promoter elements recognized by pathogenic TALEs improves disease
44 resistance without affecting plant characteristics in citrus and rice (Peng et al., 2017;
45 Xu et al., 2019). *CsLOB1* is a citrus canker S gene and plays a key role in promoting
46 pathogen growth and blistering pustule formation. Deletion of the EBE_{PthA4} sequence
47 from the *CsLOB1* gene promoter by CRISPR/Cas9 has conferred high resistance to
48 citrus canker (Peng et al., 2017). Sugars will eventually be exported transporters
49 (*SWEET*) genes are the other best-known S genes encoding sugar transporters. Some

50 *SWEET* genes can be hijacked by pathogenic bacteria to induce sucrose transport from
51 the interior of plant cells to the apoplasts and provide carbon sources for the bacteria.
52 Disruption of EBEs in promoters of three major target rice *SWEET* genes by
53 CRISPR-Cas9 avoids recognition by TALEs from *Xanthomonas oryzae* pv. *oryzae*
54 (*Xoo*) and improves bacterial blight resistance (Xu et al., 2019).

55 Generally, *Xam* contains 1-5 TALEs which determine its virulence (Bart et al.,
56 2012). TALE20 contributes toward most of the aggressiveness and virulence of *Xam*
57 in cassava (Cohn et al., 2014) by targeting a *SWEET* gene. *MeSWEET10a* expression
58 rapidly increases after infection with Xam_{TALE20} (*Xam* containing TALE20) which
59 induces sucrose translocation to the infection site and facilitates the multiplication and
60 spread of *Xam* in susceptible cassava varieties, but not in resistant varieties (Mora et
61 al., 2019). *Xam668* is a highly virulent *Xam* strain to cassava which contains five
62 TALEs including TALE20 (Bart et al., 2012). TALE20 disruption in *Xam668*
63 (*Xam668ΔTAL20*) reduces cassava water-soaking symptom development, while
64 reintroducing TALE20 into the plasmid-cured strain fully complemented the
65 symptom defect phenotype (Cohn et al., 2014). $\mathrm{TALE20}_{Xam668}$ has 20 RVDs, and
66 directly targets the EBE in the *MeSWEET10a* promoter (Cohn et al., 2014). Thus,
67 editing the EBE in the *MeSWEET10a* promoter may potentially confer resistance to
68 CBB in cassava (Lin et al., 2019).

69 *Xam11* is a highly pathogenic subspecies from Hainan, China that infects the
70 cassava SC8 cultivar with marked pathogenic symptoms (Figure S1). In this study, the
71 effect of genetically modifying the EBE in the *MeSWEET10a* promoter on CBB
72 resistance in cassava after *Xam11* infection was investigated. *TALE20* was cloned
73 based on the genome sequencing information of *Xam11*. $\mathrm{TALE20}_{Xam11}$ (TALE20 in
74 *Xam11*) has 20 RVD with variable amino acids at positions 12 and 13 in each repeat
75 (Figure S2). The promoter sequence of *MeSWEET10a* in SC8 cassava was cloned,
76 which is identical to the reported sequence in Mora et al. (2019). $\mathrm{EBE}_{\mathrm{TALE20}}$ is
77 targeted by $\mathrm{TALE20}_{Xam11}$ and is located in the -92 to -112 bp region before the

78 *MeSWEET10a* start codon (Figure S3). The dual luciferase reporter assay
79 demonstrated that TALE20$_{Xam11}$ activated the *MeSWEET10a* promoter and initiated
80 downstream expression of firefly luciferase; however, TALE20$_{Xam11}$ could not activate
81 the *MeSWEET10a* promoter lacking the EBE$_{TALE20}$ region (Figure 1A).
82 CRISPR-P v2.0 was used to design the sgRNA
83 (TGGGCGAGAAGCGTTTATAT**AGG**) targeting EBE$_{TALE20}$ based on the sequence
84 characteristics of the *MeSWEET10a* promoter in SC8 cassava. The
85 pCAMBIA1301-Cas9-EBE-sgRNA plasmid was constructed and transformed into the
86 SC8 cassava genome by *Agrobacterium*-mediated fragile embryonic callus (EFC)
87 transformation. In total, 57 independent transgenic lines were regenerated after
88 hygromycin (20 μg/mL) selection and confirmation by PCR analysis for the *Cas9*
89 gene (Figure S4). The EBE$_{TALE20}$ regions from all the transgenic lines subjected to
90 Sanger sequencing and high throughput tracking of mutation (Hi-TOM) sequencing
91 (Figure S5, Table S1) showed that Cas9 activity efficiency was 98.2%. Three types of
92 mutations were obtained among the transgenic lines: homozygous mono-allelic
93 (19.30%), homozygous bi-allelic (61.40%), and heterozygous (17.54%) (Table S1).
94 The EBE$_{TALE20}$ regions in the four mutant types of transgenic cassava (#1, #2, #3, #4)
95 and wild type SC8 cassava (WT) were shown in Figure 1B. The effects of EBE$_{TALE20}$
96 modification on *MeSWEET10a* expression in the mutant cassava lines were
97 investigated after inoculation with *Xam11*. The relative expression level of
98 *MeSWEET10a* in mutant lines showed no obvious difference from that of the wild
99 type at 0 and 0.5 day post-inoculation (dpi); however, markedly lower levels were
100 observed in mutant lines compared with that of the wild type at 1–7 dpi (Figure 1C).
101 This showed that EBE$_{TALE20}$ mutations repressed *MeSWEET10a* expression after
102 *Xam11* infection. Wild type had obvious water-soaked symptoms at 3 dpi which were
103 not observed in mutant lines (#1, #2, #3, #4). At 7 dpi, the wild type had obvious
104 pustule symptoms while the mutant lines showed slightly water-soaked symptoms; at
105 14 dpi, the wild type injection sites were withered and turned yellow, while the

106 mutant injection sites started to wither and the plaque expanded slowly; at 40 dpi,
107 whole leaves of the wild type were withered and become yellow whereas the leaves of
108 the mutant lines only withered near the plaques (Figure 1D). Diseased lesions in
109 mutant lines were significantly smaller at 3 dpi, 7 dpi, and 14 dpi (Figure 1E)
110 suggesting that EBE_{TALE20} mutations limited the expansion of CBB symptoms in
111 cassava. The bacterial growth assay showed that *Xam11* populations in the four
112 mutant lines were significantly smaller than that in the wild type at 3 dpi and 7 dpi
113 (Figure 1F). Callose is deposited on the cassava cell wall during the early stages of
114 *Xam* pathogen attack which restricts pathogen growth (Wei et al., 2021). The leaves
115 of the mutant cassava lines displayed significantly more callose depositions at 3 dpi
116 than that in the wild type (Figure 1G). These results revealed that EBE_{TALE20}
117 modification of *MeSWEET10a* in the four edited cassava lines had strong and stable
118 resistance to CBB.

119 There were no significant differences in tuber root traits and starch content
120 between the EBE_{TALE20} mutated cassava lines and the wild type plants when grown
121 under normal conditions (Figure 1H and 1I). This indicated that the EBE_{TALE20}
122 mutation in the *MeSWEET10a* promoter has no effect on yield-related traits in
123 cassava.

124 In conclusion, editing of the promoter in the disease-susceptibility gene
125 *MeSWEET10a* of SC8 cassava confers resistance to CBB. All mutated cassava lines
126 had normal morphological and yield-related traits as the wild type. The results lay a
127 research foundation for breeding cassava resistant to bacterial blight.

128

SUPPLEMENTAL INFORMATION

Supplemental Information is available at *Molecular Plant* Online.

FUNDING

This work was supported by grants from the National Key R&D Program of China (2019YFD1001105), the Hainan Provincial Natural Science Foundation of China (320RC492), and the Earmarked Fund for China Agriculture Research System (CARS-11-HNGJC, CARS-11-HNCYH).

AUTHOR CONTRIBUTIONS

Y.Y., J.G., and Y.C. designed the experiments. Y.W., M.G., R.P., X.Z., R.L., and J.L. performed the experiments. T.Z. and Y.C. conducted the cassava transformation. Y.Y., Y.W., M.G., and R.P. analyzed the data and wrote the manuscript. J.G. and Y.C. revised the manuscript. All authors read and approved the final manuscript.

ACKNOWLEDGEMENTS

The authors declare no conflict of interest.

REFERENCES

Bart, R., Cohn, M., Kassen, A., McCallum, E.J., Shybut, M., Petriello, A., Krasileva, K., Dahlbeck, D., Medina, C., Alicai, T., et al. (2012). High-throughput genomic sequencing of cassava bacterial blight strains identifies conserved effectors to target for durable resistance. Proceedings of the National Academy of Sciences of the United States of America **109**:E1972-E1979. https://doi.org/10.1073/pnas.1208003109.

Boch, J., and Bonas, U. (2010). *Xanthomonas* AvrBs3 family-type III effectors: discovery and function. Annual Review of Phytopathology **48**:419-436.

155 https://doi.org/10.1146/annurev-phyto-080508-081936.

156 **Cohn, M., Bart, R.S., Shybut, M., Dahlbeck, D., Gomez, M., Morbitzer, R.,**
157 **Hou, B.-H., Frommer, W.B., Lahaye, T., and Staskawicz, B.J.** (2014).
158 *Xanthomonas axonopodis* virulence is promoted by a transcription activator-like
159 effector–mediated induction of a SWEET sugar transporter in cassava. Molecular
160 Plant-Microbe Interactions **27**:1186-1198.
161 https://doi.org/10.1094/MPMI-06-14-0161-R.

162 **Gomez, M.A., Lin, Z.D., Moll, T., Chauhan, R.D., Hayden, L., Renninger, K.,**
163 **Beyene, G., Taylor, N.J., Carrington, J.C., and Staskawicz, B.J.** (2019).
164 Simultaneous CRISPR/Cas9‐mediated editing of cassava eIF 4E isoforms nCBP‐1
165 and nCBP‐2 reduces cassava brown streak disease symptom severity and incidence.
166 Plant Biotechnology Journal **17**:421-434. https://doi.org/10.1111/pbi.12987.

167 **Lin, Z.J.D., Taylor, N.J., and Bart, R.** (2019). Engineering disease-resistant
168 cassava. Cold Spring Harbor Perspectives in Biology **11**:a034595.
169 https://doi.org/10.1101/cshperspect.a034595.

170 **McCallum, E.J., Anjanappa, R.B., and Gruissem, W.** (2017). Tackling
171 agriculturally relevant diseases in the staple crop cassava (*Manihot esculenta*).
172 Current Opinion in Plant Biology **38**:50-58. https://doi.org/10.1016/j.pbi.2017.04.008.

173 **Mora, R.E., Rodriguez, M.A., Gayosso, L.Y., and López, C.E.** (2019). Using
174 *in vitro* plants to study the cassava response to *Xanthomonas phaseoli* pv. *manihotis*
175 infection. Tropical Plant Pathology **44**:423-429.

176 https://doi.org/10.1007/s40858-019-00296-x.

177 **Peng, A., Chen, S., Lei, T., Xu, L., He, Y., Wu, L., Yao, L., and Zou, X.** (2017).
178 Engineering canker‐resistant plants through CRISPR/Cas9‐targeted editing of the
179 susceptibility gene CsLOB1 promoter in citrus. Plant Biotechnology Journal
180 **15**:1509-1519. https://doi.org/10.1111/pbi.12733.

181 **Wang, Y., Cheng, X., Shan, Q., Zhang, Y., Liu, J., Gao, C., and Qiu, J.-L.**
182 (2014). Simultaneous editing of three homoeoalleles in hexaploid bread wheat confers
183 heritable resistance to powdery mildew. Nature Biotechnology **32**:947-951.
184 https://doi.org/10.1038/nbt.2969.

185 **Wei, Y., Zeng, H., Liu, W., Cheng, X., Zhu, B., Guo, J., and Shi, H.** (2021).
186 Autophagy‐related genes serve as heat shock protein 90 co-chaperones in disease
187 resistance against cassava bacterial blight. The Plant Journal: for Cell And Molecular
188 Biology **107**:925-937. https://doi.org/10.1111/tpj.15355.

189 **Xie, K., and Yang, Y.** (2013). RNA-guided genome editing in plants using a
190 CRISPR–Cas system. Molecular Plant **6**:1975-1983.
191 https://doi.org/10.1093/mp/sst119.

192 **Xu, Z., Xu, X., Gong, Q., Li, Z., Li, Y., Wang, S., Yang, Y., Ma, W., Liu, L.,**
193 **Zhu, B., et al.** (2019). Engineering broad-spectrum bacterial blight resistance by
194 simultaneously disrupting variable TALE-binding elements of multiple susceptibility
195 genes in rice. Molecular Plant **12**:1434-1446.
196 https://doi.org/10.1016/j.molp.2019.08.006.

Zaidi, S.S.-e.-A., Mukhtar, M.S., and Mansoor, S. (2018). Genome editing: targeting susceptibility genes for plant disease resistance. Trends in Biotechnology **36**:898-906. https://doi.org/10.1016/j.tibtech.2018.04.005.

201 **Figures**

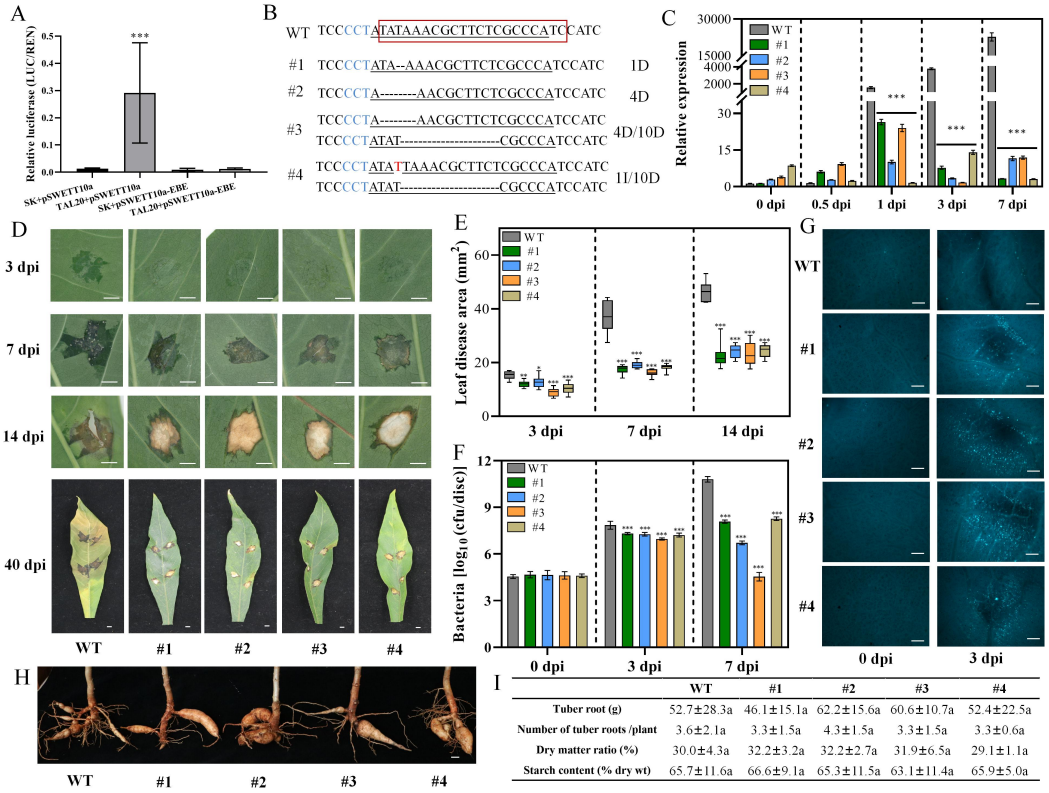

	WT	#1	#2	#3	#4
Tuber root (g)	52.7±28.3a	46.1±15.1a	62.2±15.6a	60.6±10.7a	52.4±22.5a
Number of tuber roots /plant	3.6±2.1a	3.3±1.5a	4.3±1.5a	3.3±1.5a	3.3±0.6a
Dry matter ratio (%)	30.0±4.3a	32.2±3.2a	32.2±2.7a	31.9±6.5a	29.1±1.1a
Starch content (% dry wt)	65.7±11.6a	66.6±9.1a	65.3±11.5a	63.1±11.4a	65.9±5.0a

202

203 **Figure 1. Engineering CBB resistant plants through CRISPR/Cas9-targeted**
204 **editing of the *MeSWEET10a* promoter in cassava. (**A) TALE20$_{Xam11}$ directly
205 activates *MeSWEET10a* expression through the EBE region. *MeSWEET10a*
206 promoter-luciferase fusion and 35S-driven TALE20$_{Xam11}$ constructs were delivered
207 into *Nicotiana benthamiana* cells through infection by *Agrobacterium tumefaciens*.
208 Luciferase activity was quantified after 1 dpi. SK: pGreen II62-SK vector (control
209 vector); TAL20: pGreen II62-SK-TAL20$_{Xam11}$ vector; pSWEET10a: pGreen
210 II0800-pMeSWEET10a-LUC vector; pSWEET10a-EBE: pGreen
211 II0800-pMeSWEET10a-EBE$_{TAL20}$-LUC vector (deletion of EBE$_{TAL20}$ from the
212 *MeSWEET10a* promoter). Data are displayed as mean technical replicates ± standard
213 deviation. Experiments were repeated three times with similar results (Student's t-test,
214 ***P < 0.005). **(B)** Hi-TOM sequencing of the EBE$_{TALE20}$ regions of wild type (WT)
215 non-transgenic SC8 cassava compared with the engineered lines #1, #2, #3, and #4.
216 The EBE$_{TALE20}$ region of the TALE20$_{Xam11}$ target is marked in a red box in WT; the
217 sgRNA sequences are underlined; the protospacer adjacent motif (PAM) sites are

218 marked in blue text; the hyphens are missing bases, and the red letter is the inserted
219 base. **(C)** Time course of *MeSWEET10a* expression in mutant lines and WT after
220 *Xam11* inoculation. *MeSWEET10a* transcript levels in leaves determined by qPCR at
221 0, 0.5, 1, 3, and 7 dpi. Three biological repeats were performed for each data point
222 (Student's t-test, ***P < 0.005). **(D)** Symptom development after *Xam11* inoculation.
223 Scale bar, 5 mm. **(E)** and **(F)** Time course of leaf disease areas and bacterial numbers
224 after *Xam11* inoculation. At least 10 leaves were harvested for the diseased areas with
225 the bacterial number assay performed using three biological replicates (Student's
226 t-test, *P < 0.05, ***P < 0.005). (**G**) Callose depositions in leaves. Scale bar, 50 μm.
227 **(H)** Tuber root phenotypic characterizations. Scale bar, 1 cm. **(I)** Yield-related traits
228 shown as the mean ± SD from five plants of each line. *P* values were calculated using
229 Student's t-test. The values marked with the same letter (a) represented no significant
230 difference.
231

232 **Supplemental Figures**

233

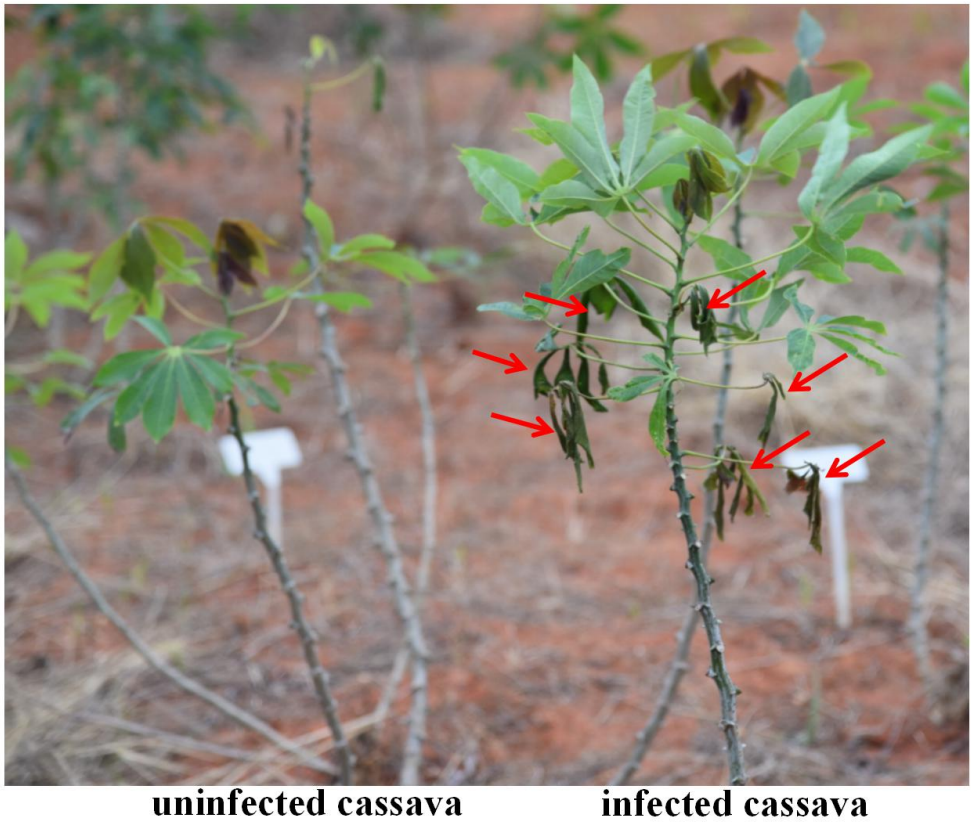

234

235 **Figure S1. *Xam11* infects cassava cultivar SC8 with marked pathogenic**

236 **symptoms.** Red arrows indicate the region affected in the infected cassava.

237

MDPIRPRTPSPAHELLAGPQPDRVQPQPTADRGGAPPAGSPLDGLPARRTMSRTRLPSPPAPLPAFSAGSFSD
LLRQFDPSLLDTSLFNSMSAFGAPHTEAASGEGDEVQSGLRAADDPQATVQVAVTAARPPRAKPAPRRRA
AHTSDASPAGQVDLCTLGYSQQQQEKIKLKARSTVAQHHEALIGHGFTRAHIVALSQHPAALGTVAVKYQ
AMIAALPEATHEDIVGGGKQWSGARALEALLTVSGELRGPPLQLDTGQLLKIAKRGGVTAVEAVHAWRN
ALTGAPLN

20 Repeat variable diresidues (RVD)

LTPDQVVAIASNIGGKQALETVQRLLPVLCEQHG
LTLDQVVAIASNGGGKQALETVQRLLPVLCEQHG
LTPDQVVAIASNIGGKQALETVQRLLPVLCEQHG
LTPDQVVAIASNNGGKQALETVQRLLPVLCEQHG
LTRAQVVAIASNGGGKQALETVQRLLPVLRQAHG
LTPAQVVAIASHDGGKQALETVQQLLPVLCEQHG
LTPAQVVAIASNNGGKQALETVQRLLPVLRQAHG
LTPDQVVAIASHDGGKPALETVQRLLPVLCEQHG
LTPDQVVAIASNNGGKPALETVQRLLPVLCEQHG
LTRAQVVAIASNGGGKQALETVQRLLPVLRQAHG
LTPAQVVAIASHDGGKQALETVQQLLPVLCEQHG
LTPAQVVAIASNSGGKQALETVQRLLPVLCEQHG
LTPDQVVAIASHDGGKQALETVQRLLPVLCEQHG
LTPDQVVAIASNNGGKQALETVQRLLPVLCEQHG
LTPDQVVAIASHDGGKQALETVQRLLPVLCEQHG
LTPDQVVAIASHDGGKQALETVQRLLPVLCEQHG
LTPDQVVAIASHDGGKQALETVQRLLPVLRQAHG
LTPDQVVAIASNIGGKQALETVQRLLPVLCEQHG
LTPDQVVAIASNGGGKQALETVQRLLPVLCEQHG
LTPAQVVAIASNGGGRPALE

SIFAQLSRPDQALAALTNDHLVALACLGGRPALEAVKKGLPHAPTLIKRTNRRLPERTSHRVADHAQVARVL
GFFQCHSHPAQAFDEAMTQFGMSRHGLLQLFRRAGVTELEAHSGTLPPASQRWHRILQASGMKRAEPSG
ASAQTPDQASLHAFADALERELDAPSPIDRAGQALASSS**RKRSRS**ESSVTGSFAQQAVEVRVPEQRDALHF
LPLSW**GVKRPR**TRIGGGLPDPGTPMDADLAASSTVMWEQDADPFAGAADDFPAFNEEEMAWLMELFPQ

Nuclear localization Signals (NLS)

Acidic activation domain (AAD)

Figure S2. Analysis of TALE20 protein sequence from *Xam11*. TALE20$_{Xam11}$ has 20 RVD with variable amino acids at positions 12 and 13 in each repeat (highlighted in red).

AACTTTTAGAATGAGCCCTTGAAATGAAACCTCTAAGCTTGTAGGTTCTAATAGGGT
TACTTAATTAAATGATAGACCTAACCCTTATAATTTGATTATGACTTTTTATAATAG
AGATGAACGAAACCACAAAATTCTCCAGTTACCCAATAAACGTGGGAATGAGAGTGT
GTGGTTAGGAATCCATGTGCATGGCAAGAGAGAAAATCACAGGACTTTCTTTCAAAT
TAATTCTTGGTTAATCATGATTACATATTAATCACCTTGTCTTTTACGTGCAATCTT
CAAGTTTTTCAACCATTATTAATTACGTTGTGGACGTGGACAACTTGGAAGAAATCG
TAAAGGGCCGTCAACAAGCATTCACAAGAGCTGTTATCAGCGAGGGGGAATGAGACA
ACGGCGGCTGATGTGTTATGGTGGTAAACTGGGAAATACTAGGCACGGTTTCTTGTA
TGGGAAAAACAGCATATCCTCTGCCATGATGCTGAGCTCGTTTCTCCACCGTTTGAT
TGAATGTTCTGATTTGTTTCATCATCATCAAATGCGATTACACATCAGAAAGCTTGT
TGATGGGATTCTGTAACAAATGAAGTAAGCTTCAAAGCCTTTTGGATCCCTACTATG
GGAATGATCCAAGTGGGTTAACTACTATTAGTTAGTTGACCTCATCCACTGCGCTAT
AGGCTCATATAGGTCCAGTTAACTCGATCTCTGAAATTAAATTTCTATTTTTTAAAT
GAAATTAAGTCAAATGCATTATACGTACCCTTCCTCAACACCCTATATTATATTAAC
AAAAATCTTTATATTGCATTGCATCCAGTAAAATGATAAAAAAAAAATCAGGGTATA
ATTTTCTTAATCCATGCATGATAATCTGATTCATTTCATGTATAAATTTAAATATAA
TTTGTTGAGAAAGAGCAGGAGTCCTCTGGAACTAAAATATGAGTTGTAACCCTTAAA
ACCACTTGGTGGGTGACACATCAGAAAGAACAAAGTGGGACCCTTTGAATTTTGTGC
ACGTACTAGGAATGGTACCTACAAGTAGGGCTACTTTTGTATAGTGAGAGTTTACCT
GAAGAAAAATTAACCATAGATGGATAAATATAGGGCATTAGGTTTAGAAAGCTGTTC
GGATCATTTTAACGTAAAAAGCACTTAGTAGGACCAACTTAAAAGTAACCATAAAAT
TAATATTGTTTTCTCTTTCTTCAAAAAAAATAATAAAAGAAACAAGGCCACTGTTAC
ATTGACATATTTTATTCACTTTAATCATGCATGCAACTTGACTTCATTCCGTTCCCT
GGATTCCTCCCCT**ATATAAACGCTTCTCGCCCA**TCCATCATTGCACAACATAGC
TAGAGTTTCCTCTTGAGAAAGAGAGTTTCCTCTGCACAAGGGAAAGAGAGTCTCTAC
TATAGCCGGAGAA**ATG**GCCTTGCACTTGTCATTGGACTTCGTTTTTGGCGTTTTAGG
TACTA

Figure S3. *MeSWEET10a* promoter sequence. EBE_{TALE20} (bold letters) is located in the -92 to -112 bp region before the start codon (red letters) of *MeSWEET10a*, which is recognized by $TALE20_{Xam11}$.

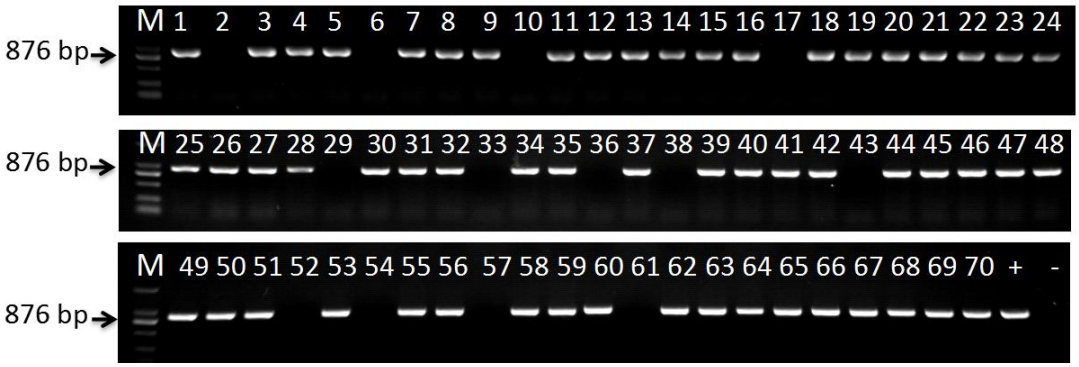

Figure S4. Transgenic lines confirmed by PCR analysis of the *Cas9* gene. M: DL2000 marker; 1-70, transgenic lines; +, positive control; -, negative control. 13, 23, 19, and 20 represent mutant lines #1, #2, #3, and #4.

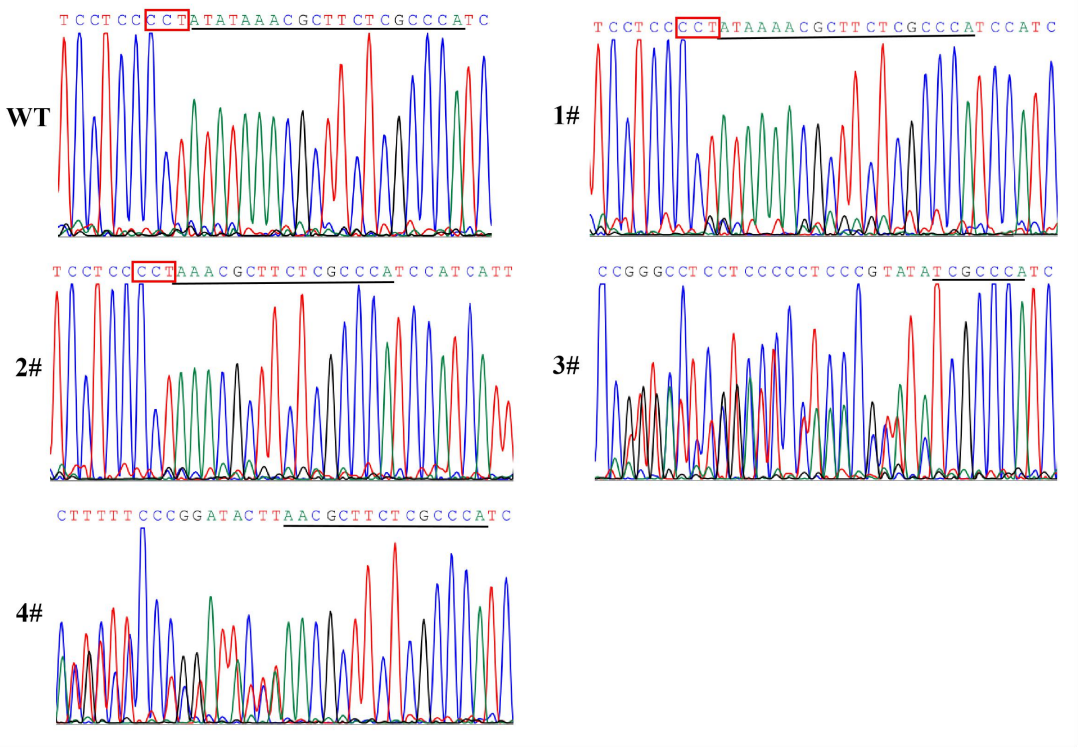

Figure S5. Sanger sequencing peak map of target fragments in mutant lines #1, #2, #3, #4 and wild type (WT). Red boxes represent the protospacer adjacent motif (PAM), and underlines represent the target sequences.